Optimization-based Synthesis of Time-Modulated Arrays with Accurate Time-Frequency Analysis

Lorenzo Poli[1], Marco Salucci[1], Diego Masotti[2], and Paolo Rocca[1]
[1] ELEDIA Research Center (ELEDIA@UniTN – University of Trento), Via Sommarive 9, 38123 Trento – Italy
{lorenzo.poli, marco.salucci, paolo.rocca}@eledia.org
[2] Department of Electrical, Electronic, and Information Engineering, University of Bologna, 40136 Bologna – Italy
diego.masotti@unibo.it

***Abstract*— The synthesis of time-modulated arrays (*TMA*s) is carried out by means of a customized implementation of the Particle Swarm Optimization (*PSO*), carefully taking into account in the analysis block the non-linear characteristics of the radio-frequency (*RF*) switches used in antenna beam-forming network and the mutual coupling effects between the array elements. A set of numerical results are reported and discussed in a comparative fashion with those obtained with a state-of-the-art method limited to deal with ideal *TMA*s.**

***Keywords*— time-modulated linear arrays, particle swarm optimization, harmonic balance, directivity optimization.**

I. Introduction

Four-dimensional (*4D*) arrays are unconventional antennas in which one or more of their parameters are subject to modulation in time-domain [1]. Beyond theoretical studies [2]-[4], several methods have been proposed since the beginning of the millennium, aimed at profitably exploiting this additional degree of freedom and suitably handling the spurious radiation generated in sideband (the so called sideband radiation, *SR*), mainly based on stochastic single-objective (e.g., differential evolution, *DE* [5], particle swarm optimization, *PSO* [6], genetic algorithms, *GA* [7], and simulated annealing, *SA* [8]) or multi-objective (e.g., multiobjective evolutionary algorithm based on objective decomposition, *MOEA/D* [9], and multiobjective particle swarm optimization, *MOPSO* [10]) optimizations. Several works have been also presented to investigate the possibility to employ the *TMA*s in different applicative frameworks, among which wireless power transmission (*WPT*) [11], direction of arrival estimation (*DoA*) [12], radar [13] and communications [14, 15].

Dealing with radar or communications, as already discussed in [16]-[18], the time-varying behavior caused by the dynamic on/off switching of the array elements can significantly compromise the reliability of the system if the antenna directivity along the beam pointing angle has to be preserved. In order to limit these drawbacks, a strategy for properly optimizing the switching sequence to keep constant the instantaneous directivity of the main beam has been presented in [16]. However, although effective, such strategy deals with isotropic elements without taking into account the coupling effects between the radiating elements and the non-ideal behavior of the *RF* switches. In order to solve these issues, this paper presents a novel approach based on particle swarm optimization to determine the pulse sequences exciting the array elements, enhanced by the harmonic balance (*HB*) technique. Such technique has been already presented in [19, 20] to accurately analyze the field radiated by the *TMA*, but in this contribution and unlike [19, 20], it will be directly integrated within an optimization procedure.

This work benefited from the networking activities carried out within the project "CYBER-PHYSICAL ELECTROMAGNETIC VISION: Context-Aware Electromagnetic Sensing and Smart Reaction (EMvisioning)" funded by the Italian Ministry of Education, University, and Research within the PRIN2017 Program, the SNATCH project (2017-2019) funded the Italian Ministry of Foreign Affairs and International Cooperation, Directorate General for Cultural and Economic Promotion and Innovation, and the project "SMARTOUR - Piattaforma Intelligente per il Turismo" (Grant no. SCN_00166) funded by the Italian Ministry of Education, University, and Research within the Program "Smart cities and communities and Social Innovation".

II. Mathematical Formulation

Let us consider a linear array of N radiating elements aligned and equally-spaced (by distance d) along the z-axis of a conventional coordinate system. Assuming that each element of the array is excited by an independent pulsed periodic function of period T_p

$$I_n(t)=\begin{cases}1, & t_n^{on}<t<t_n^{off}\\ 0, & elsewhere\end{cases}, \quad n=1,...,N, \tag{1}$$

with switch-on and switch-off instants t_n^{on} and t_n^{off}, respectively, generated through the commutation of a set of RF switches inserted in the feeding network, the arising radiated field can be expressed as

$$\mathbf{E}(\mathbf{r},t)=e^{j2\pi f_0 t}\sum_{n=1}^{N} I_n(t)\mathbf{E}_n(\mathbf{r})e^{j\beta(n-1)d\cos\theta}, \tag{2}$$

where $\beta=2\pi/\lambda_0$ is the wave-number corresponding to the working frequency f_0, λ_0 being the wavelength, and $\mathbf{E}_n(\mathbf{r})$ is the active element pattern of the n-th element, $n=1,...,N$, computed by exciting a single-radiator with all others terminated with matched loads. Taking advantage of the harmonic balance (*HB*) technique [19, 20], the field radiated by the *TMA* is accurately analyzed by means of the cascade of linear and nonlinear sub-networks described in the frequency and time domain, respectively. In order to avoid significant fluctuations in the array instantaneous directivity and then undesired amplitude modulations in the transmitted/received signal due to the varying of the number of active elements within the modulation period, the on-off sequences of the pulses controlling the *RF* switches are optimized. Accordingly, two different approaches are adopted: (*i*) a *bounded* approach and (*ii*) a *full* approach. Dealing with (*i*), the pulse durations which allow for the generation of a beam pattern at the carrier frequency with desired sidelobe level are defined by means of an analytic method, whereas the rising instants of the rectangular pulses

978-9-0827-9703-9/19/$31.00 ©2019 IEEE

are optimized through a *PSO*, via minimization of the following objective function:

$$\Psi_B^{(k)}(\boldsymbol{\tau}_B^{(k)}) = \frac{1}{\overline{D}(\boldsymbol{\tau}_B^{(k)}) \times S} \sum_{s=1}^{S} \left| \overline{D}(\boldsymbol{\tau}_B^{(k)}) - D(t_s; \boldsymbol{\tau}_B^{(k)}) \right| \tag{3}$$

where $\boldsymbol{\tau}_B = \left\{ t_n^{on}; n = 1,..., N \right\}$ is the vector of the optimized parameters at the k-th iteration of the process (K being the maximum number of iterations), $t_s = T_p(s-1)/S$ is the s-th time sample (S being the total number of samples within a period T_p) at which the directivity is evaluated as

$$D = \frac{\max_\theta \left| \mathbf{E}(\theta) \right|^2}{\frac{1}{2} \int_0^\pi \left| \mathbf{E}(\theta) \right|^2 \sin\theta d\theta} \tag{4}$$

and $\overline{D}$ is the average directivity over a modulation period.

Dealing with the *full* approach, both the rising and falling instants (i.e., t_n^{on} and t_n^{off}, $n = 1,..., N$) of the rectangular pulses are optimized through the stochastic algorithm, minimizing the following objective function

$$\Psi_F^{(k)}(\boldsymbol{\tau}_F^{(k)}) = \alpha_D \Psi_B^{(k)}(\boldsymbol{\tau}_F^{(k)}) + \alpha_{SLL} H\left[SLL^{(k)}(\boldsymbol{\tau}_F^{(k)}) - SLL^{des} \right] \frac{\left| SLL^{(k)}(\boldsymbol{\tau}_F^{(k)}) - SLL^{des} \right|^2}{\left| SLL^{des} \right|^2} + \alpha_{BW} H\left[BW^{(k)}(\boldsymbol{\tau}_F^{(k)}) - BW^{des} \right] \frac{\left| BW^{(k)}(\boldsymbol{\tau}_F^{(k)}) - BW^{des} \right|^2}{\left| BW^{des} \right|^2} \tag{5}$$

where $\boldsymbol{\tau}_F = \left\{ t_n^{on}, t_n^{off}; n = 1,..., N \right\}$ is the new vector of the optimized parameters, $H[\cdot]$ is the Heaviside function, *SLL* is the sidelobe level, *BW* is the half-power beamwidth (the superscript $\cdot^{des}$ indicates the target values for both *SLL* and *BW*) and α_{SLL}, α_{HPBW} and α_D are real weighting coefficients.

III. Numerical Results

In this section, in order to assess the effectiveness of the proposed synthesis method, a comparison between the results obtained with and without exploiting the *HB* technique during the optimization process is presented: these two approaches will be identified as "*HB-PSO*" and "*PSO*" in the following (in the second case, the optimization is carried out with a standard approach considering isotropic elements and ideal *RF* switches [16], but at the end of the optimization process the solution is analyzed by means of the *HB* technique). Toward this aim, a linear array composed by $N = 16$ printed monopoles and their microstrip feeding network is considered, whose *RF* switches are assumed to be controlled by symmetric pulse sequence. The monopoles, equally-spaced by 0.5λ and resonating at $2.45GHz$, are realized on a 0.635mm-thick substrate with dielectric permittivity ε_r=6.15 (tanδ=0.0028). The optimization parameters of the *PSO* have been set as follows: swarm dimension $P = N$, $K = 200$, inertial weight $w = 0.4$, cognitive and social acceleration coefficients $C_1 = C_2 = 2.0$ and unitary weighting coefficients $\alpha_D = \alpha_{SLL} = \alpha_{BW} = 1.0$.

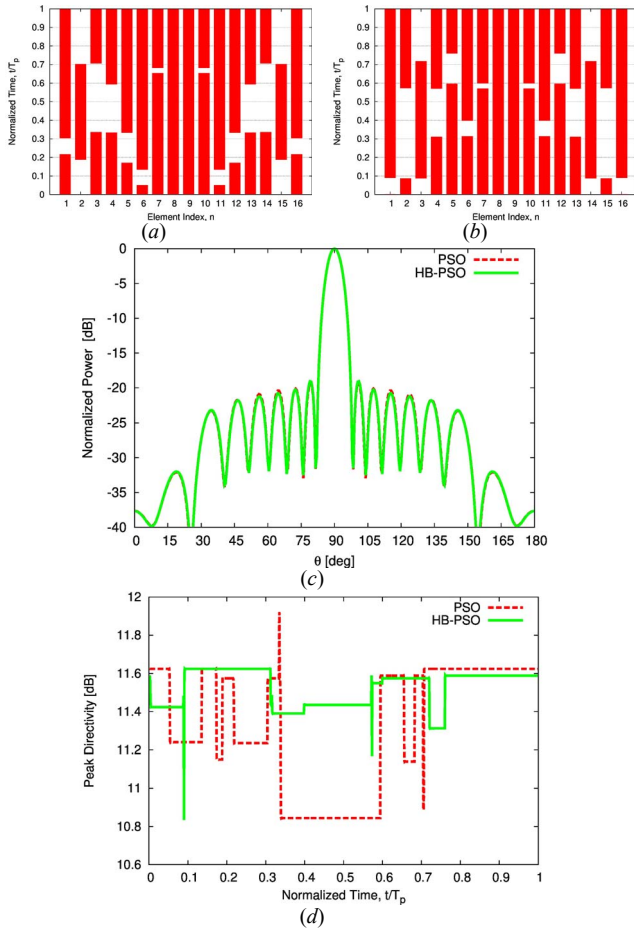

Fig. 1. *Bounded Approach* – (*a*)(*b*) Pulse sequences optimized through (*a*) the *PSO* and (*b*) the *HB-PSO* methods along with (*c*) the corresponding radiation patterns and (*d*) the peak directivity function within a modulation period.

TABLE I. Bounded Approach: Statistic of Peak Directivity within a Modulation Period.

	avg[*D*]	var[*D*]	min[*D*]	max[*D*]
PSO	11.33	1.06×10^{-1}	10.84	11.92
HB-PSO	11.52	9.66×10^{-3}	10.83	11.63

Dealing with bounded approach, the pulse durations have been defined in order to generated a Dolph-Chebyshev pattern with sidelobe level equal to $SLL = -20\,dB$ at the central frequency. The pulse sequences with optimized pulse shifts obtained through the *PSO* and the *HB-PSO* methods are depicted in Fig. 1(*a*) and Fig. 1(*b*), respectively, whereas the corresponding radiation patterns are shown in Fig. 1(*c*). Although such patterns are almost perfectly overlapped because of using the same pulse durations, the behavior of the directivity peak vs. time of the two solutions turns out to be significantly different. More in detail, it is possible to notice from Fig. 1(*d*) that a high average peak directivity and a lower variance is obtained through the *HB-PSO* method as confirmed by the data reported in Tab. I: $\text{avg}[D]\big|_{HB-PSO} = 11.52\,dB$ vs. $\text{avg}[D]\big|_{PSO} = 11.33\,dB$ and $\text{var}[D]\big|_{HB-PSO} = 9.66\times10^{-3}\ dB$ vs. $\text{var}[D]\big|_{PSO}$

$= 1.06 \times 10^{-1}\, dB$. In the second numerical example, the performance of the *HB-PSO* are investigated using the full approach, and the target sidelobe level and beamwidth of the pattern to be synthesized at the carrier frequency have been chosen as $SLL^{des} = -20\, dB$ and $BW^{des} = 7.0\,\text{deg}$ (namely, the values corresponding to those of the Dolph-Chebyshev pattern of the previous example).

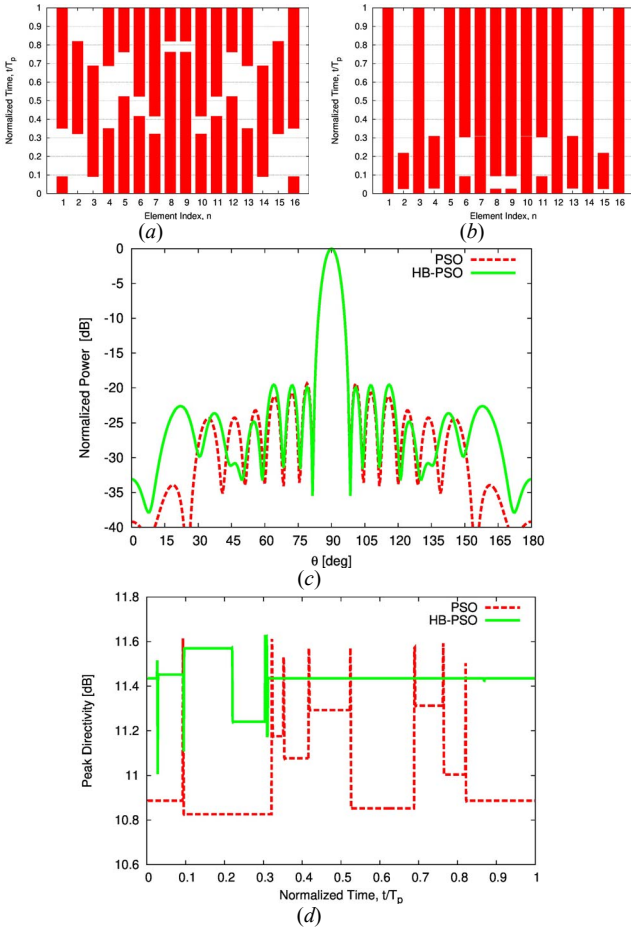

Fig. 2. *Full Approach* – (*a*)(*b*) Pulse sequences optimized through (*a*) the *PSO* and (*b*) the *HB-PSO* methods along with (*c*) the corresponding radiation patterns and (*d*) the peak directivity function within a modulation period.

TABLE II. FULL APPROACH: STATISTIC OF PEAK DIRECTIVIY WITHIN A MODULATION PERIOD.

	avg[*D*]	var[*D*]	min[*D*]	max[*D*]
PSO	10.83	3.51×10^{-2}	10.83	11.61
HB-PSO	11.44	6.05×10^{-3}	11.01	11.62

The pulse sequences fully optimized via *PSO* and *HB-PSO* are depicted in Fig. 2(*a*) and 2(*b*), respectively, and the arising radiation patterns are shown in Fig. 2(*c*). The better performance of *HB-PSO* method are confirmed also when the full approach is concerned. Indeed, as for the previous numerical example, the method guarantees high average peak directivity and lower variance, as noticeable from Fig. 2(*d*) and confirmed by the values reported in Tab. II. More precisely, $\text{avg}[D]\big|_{HB-PSO} = 11.44\, dB$ vs. $\text{avg}[D]\big|_{PSO} = 10.83\, dB$ and $\text{var}[D]\big|_{HB-PSO} = 6.05\times10^{-3}\, dB$ vs. $\text{var}[D]\big|_{PSO} = 3.51\times10^{-2}\, dB$. Moreover, a lower sidelobe level is also achieved through the *HB-PSO* ($SLL\big|_{HB-PSO} = -19.56\, dB$ vs. $SLL\big|_{PSO} = -19.40\, dB$).

IV. CONCLUSION

A novel method for optimizing the instantaneous directivity of a time-modulated linear array by means of a particle swarm optimization enhanced by an accurate time-frequency analysis aimed at taking into account the coupling phenomena between the radiating elements and the non-ideal behavior of the switches in the array feed network has been presented in this paper. Selected numerical results have shown the better performance of the proposed technique compared to a state-of-the-art method considering ideal *TMA*s. Future works will be devoted to the study of the effects of mutual impedance and active reflection coefficient in *TMA*s also focusing on the main differences with respect to conventional phased arrays.

REFERENCES

[1] P. Rocca, G. Oliveri, R. J. Mailloux, and A. Massa, "Unconventional phased array architectures and design Methodologies - A review," *Proceedings of the IEEE*, vol. 104, no. 3, pp. 544–560, March 2016.

[2] J. C. Bregains, J. Fondevila, G. Franceschetti, and F. Ares, "Signal radiation and power losses of time-modulated arrays," *IEEE Trans. Antennas Propag.*, vol. 56, no. 6, pp. 1799–1804, Jun. 2008.

[3] R. Maneiro-Catoira, J. C. Bregains, J. A. Garcia-Naya, and L. Castedo, "On the feasibility time-modulated arrays for digital linear modulations: A theoretical analysis," *IEEE Trans. Antennas Propag.*, vol. 62, no. 12, pp. 6114–6122, Dec. 2014.

[4] E. Aksoy and E. Afacan, "Calculation of sideband power radiation in time-modulated arrays with asymmetrical positioned pulses," *IEEE Antennas Wirelss Propag. Lett.*, vol. 11, pp. 133–136, 2012.

[5] S. Yang, Y. B. Gan, and A. Qing, "Sideband suppression in time-modulated linear arrays by the differential evolution algorithm," *IEEE Antennas Wireless Propag. Lett.*, vol. 1, pp. 173-175, 2002.

[6] L. Poli, P. Rocca, L. Manica, and A. Massa, "Handling sideband radiations in time-modulated arrays through particle swarm optimization" *IEEE Trans. Antennas Propag.*, vol. 58, no. 4, pp. 1408–1411, Apr. 2010.

[7] J. Euziere, R. Guinvarc'h, B. Uguen, and R. Gillard, "Optimization of sparse time-modulated array by genetic algorithm for radar applications," *IEEE Antennas Wireless Propag. Lett.*, vol. 13, pp. 161–164, 2014.

[8] J. Fondevila, J. C. Bregains, F. Ares, and E. Moreno, "Optimizing uniformly excited linear arrays through time modulation," *IEEE Antennas Wireless Propag. Lett.*, vol. 3, pp. 298–301, 2004.

[9] Y. Chen, S. Yang, and Z. Nie, "Improving conflicting specifications of time-modulated antenna arrays by using a multiobjective evolutionary algorithm," *Int. J. Numer. Model.*, vol. 25, no. 3, pp. 205–215, May 2012.

[10] W. Li, Y. Hei, J. Yang, and X. Shi, "3D pattern synthesis of time-modulated conformal arrays with a multiobjective optimization approach," *International Journal of Antennas and Propagation*, vol. 2014, pp. 1–12, 2014.

[11] D. Masotti, A. Costanzo, M. Del Prete, and V. Rizzoli, "Time-modulation of linear arrays for real-time reconfigurable wireless power transmission," *IEEE Trans. Microw. Theory Tech.*, vol. 64, no. 2, pp. 331-342, Feb. 2016.

[12] G. Li, S. Yang, and Z. Nie, "Direction of arrival estimation in time modulated linear arrays with unidirectional phase center motion," *IEEE Trans. Antennas Propag.*, vol. 58, no. 4, pp. 1105–1111, Apr. 2010.

[13] G. Li, S. Yang, and Z. Nie, "A study on the application of time modulated antenna arrays to airborne pulsed doppler radar," *IEEE Trans. Antennas Propag.*, vol. 57, no. 5, pp. 1578–1582, May 2009.

[14] R. Maneiro-Catoira, J. C. Bregains, J. A. Garcia-Naya, and L. Castedo, P. Rocca, and L. Poli, "Performance analysis of time-modulated arrays for the angle diversity reception of digital linear modulated signals," *IEEE Journal of Selected Topics in Signal Processing*, vol. 11, no. 2, pp. 247–258, Mar. 2017.

[15] J. Guo, L. Poli, M. A. Hannan, P. Rocca, S. Yang, and A. Massa, "Time-modulated arrays for physical layer secure communications: optimization-based synthesis and experimental assessment," *IEEE Trans. Antennas Propag*., vol. 66, no. 12, pp. 6939–6949, Dec. 2018.

[16] L. Manica, P. Rocca, L. Poli, and A. Massa, "Almost time-independent performance in time-modulated linear arrays," *IEEE Antennas Wireless Propag. Lett*., vol. 8, pp. 843–846, Aug. 2009.

[17] P. Rocca, L. Poli, and A. Massa, "Instantaneous directivity optimisation in time-modulated array receivers," *IET Microw. Antennas Propag*., vol. 6, no. 14, pp. 1590–1597, Nov. 2012.

[18] R. L. Haupt, "Time modulated receive arrays," *Proc. IEEE Antennas Propag. Symp.*, Jul.2011, pp. 968–971.

[19] D. Masotti, P. Francia, A. Costanzo, and V. Rizzoli, "Rigorous electromagnetic/circuit-level analysis of time-modulated linear arrays," *IEEE Trans. Antennas Propag*., vol. 61, no. 11, pp. 5465–5474, Nov. 2013.

[20] P. Rocca, D. Masotti, A. Costanzo, M. Salucci, and L. Poli, "The role of accurate dynamic analysis for evaluating time-modulated arrays performance," *IEEE Antennas Wireless Propag. Lett*., vol. 16, pp. 2663–2666, 2017.